PRIFYSGOL BANGOR / BANGOR UNIVERSITY

PRIFYSGOL
BANGOR
UNIVERSITY

Versatile Hyperbranched Poly(-Hydrazide Ester) Macromers as Injectable Antioxidative Hydrogels

Xu, Qian; Venet, Manon; WAng, Wei; Creagh-Flynn, Jack; Wang, Xi; Li, Xiaolin; Gao, Yongshenng; Zhou, Dezhong; Zeng, Ming; Lara-Saez, Irene; A, Sigen; Tai, Hongyun; Wang, Wenxin

ACS Applied materials and interfaces

Peer reviewed version

Cyswllt i'r cyhoeddiad / Link to publication

Versatile Hyperbranched Poly(β-Hydrazide Ester) Macromers as Injectable Antioxidative Hydrogels

Qian Xu[1], Manon Venet[2], Wei Wang[3], Jack Creagh-Flynn[1], Xi Wang[1], Xiaolin Li[1], Yongsheng Gao[1], Dezhong Zhou[1], Ming Zeng[1], Irene Lara-Sáez[1], Sigen A[1],*, Hongyun Tai[4], Wenxin Wang[1],*

[1] Charles Institute of Dermatology, School of Medicine, University College Dublin, Belfield, Dublin 4, Ireland.

[2] Molecular and Cellular Biology, Specialty Skin Biology, Department of Biology, Claude Bernard University Lyon I, Lyon-France.

[3] School of Materials Science and Engineering, Tianjin University, Tianjin 300350, China.

[4] School of Chemistry, Bangor University, Bangor, Gwynedd LL57 2DG, UK

Corresponding author:

    wenxin.wang@ucd.ie

    sigen.a@ucdconnect.ie

ABSTRACT: Synthetic reactive oxygen species (ROS)-responsive biomaterials have emerged as a useful platform for regulating critical aspects of ROS-induced pathologies and can improve such hostile microenvironments. Here, we report a series of new hyperbranched poly(β-hydrazide ester) macromers (HB-PBHEs) with disulfide moieties synthesized *via* an "A2+B4" Michael addition approach. The three-dimensional structure of HB-PBHEs with multi-acrylate end groups endows the macromers with rapid gelation capabilities to form (1) injectable hydrogels *via* crosslinking with thiolated hyaluronic acid, and (2) robust UV-crosslinked hydrogels. The disulfide containing macromers and hydrogels exhibit H_2O_2-responsive degradation compared to the counterparts synthesized by a dihydrazide monomer without disulfide moieties. The cell viability under a high ROS environment can be well-maintained under the protection of the disulfide containing hydrogels.
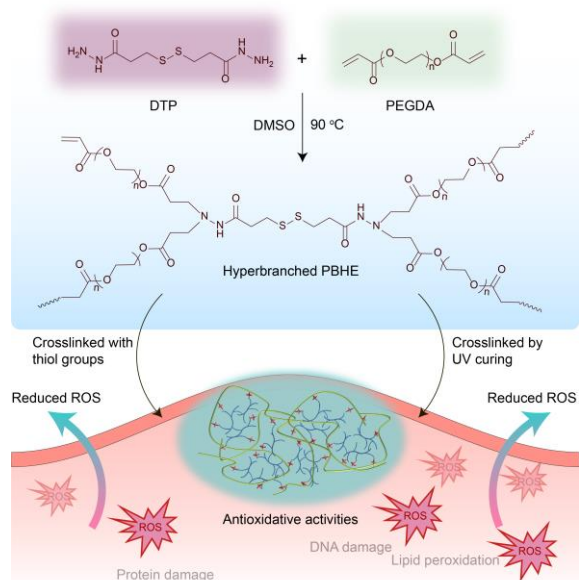
Introduction

The overexpression of reactive oxygen species (ROS) results in oxidative stress, which poses a high risk of DNA damage, mitochondrial impairment, and necrocytosis.[1] Such damages caused by harsh ROS microenvironments can lead to numerous diseases, such as cancer and inflammation-related diseases.[2,3] In order to alleviate overproduced ROSs which is harmful to the human body, antioxidants were utilized by direct local administration, however, this approach often fails due to the inhibition of bioactivity and stability of antioxidants.[4] Thus, the development of a new generation of antioxidative materials which can circumvent the abovementioned drawbacks is appealing for biomedical applications. In recent years, ROS-sensitive functional groups which respond to H_2O_2 and superoxide (O_2^-) have been reported as antioxidative components such as dopamine,[5] sulfide, disulfide, poly(thioketal), poly(propylene sulfide).[3,6] Among these functional groups, disulfides can be cleaved under mild conditions either by oxidative or reductive reaction. Disulfide bond-containing materials can function as effective radical scavenging and antioxidative components. For example, glutathione (GSH) conjugated (through disulfide bond) micelles are able to capture free radicals in 2, 2-diphenyl-1-picrylhydrazyl (DPPH) and can be used as antioxidants. The free radical can be scavenged through the single electron transfer from disulfide groups to the DPPH.[7,8] Jun Zhang *et al.* demonstrated that diallyl disulfide is able to reduce ROS production and the proinflammation cytokine levels.[9] Li-Jun Wan *et al.* reported a disulfide containing nanoparticle system for dual responsive to hydrogen peroxide and GSH, which

showed a programmable paclitaxel release.[10] Therefore, a biocompatible material containing disulfide moieties would hold great promise to improve the antioxidative therapeutic efficacy.

Among numerous biomaterials developed in recent years, hydrogel materials with high water retention rate and tunable physiochemical properties have emerged as the most promising option for biomedical applications. Several hydrogel systems incorporated with free-radical scavenging motifs have been reported and showed significantly enhanced antioxidative property.[11–14] However, some key challenges persist regarding the optimal formulation of antioxidative hydrogels, such as complicated synthetic procedures, hazardous reagents, limited and unsuitable mechanical properties, and inefficient antioxidation, leading to restricted clinical and failure of specific applications.[15]

Poly(β-amino ester)s (PBAEs), first reported by Robert Langer and co-workers,[16,17] have been widely used in the field of gene delivery[18–20] and tissue scaffold applications[21,22] due to their excellent biodegradability and biocompatibility. There has been an increasing interest in generating biocompatible PBAE smart hydrogels for tissue repair. However, most of the attention has been focused on linear PBAEs (LPBAEs), which only result in low crosslinked hydrogels with a compromised mechanical strength.[23] Hyperbranched polymers with three-dimensional structure (3D) and multi-functional end groups have shown great advantages in the formation of hydrogels for tissue engineering.[24–26] Previous studies in

Wang's group have demonstrated that highly branched PBAEs can be obtained *via* "A2+B3+C2" Michael addition

Scheme 1. Preparation of HB-PBHE macromers and fabrication of antioxidative hydrogels. HB-PBHEs are synthesized *via* "A2+B4" Michael addition approach. The hydrogels exhibit significant antioxidative effect.

polymerization by introducing branching units.[20,27–29] This approach provides great advantages over previously published methods.[20] Then, in the same lab the hyperbranched PBAEs (HB-PBAEs) were also successfully designed and synthesized *via* a single step "A2 + B4" Michael addition approach.[23] The resultant HB-PBAEs-based hydrogels exhibited adjustable mechanical properties and degradation rates, which showed a great potential in skin wound healing application. Thomas D. Dziubla *et al.* designed a branched PBAE based hydrogel incorporated with disulfide bonds.[30] The reduced hydrogel showed the significant protection to cells and mitochondria from the acute oxidative stress. However, the hydrogel was synthesized directly from the organic solvent which needs a further solvent exchanging step to remove the toxic organic solvent. The potential toxic solvent residual and tedious purification process significantly impeded the practical application. Hence, there is a pressing need to develop a facile strategy for creating hydrogel systems with a combination of both antioxidation and good biocompatibility.

In this report, we demonstrate that two new classes of hyperbranched poly(β-hydrazide esters) (HB-PBHEs) macromers were achieved using "A2 + B4" Michael addition approach. Poly(ethylene glycol) diacrylates (PEGDA) with different molecular weights were selected as A2, and two dihydrazide monomers were used as B4, namely 3,3'-dithiobis(butanoic hydrazide) (DTP) and suberic dihydrazide (SDH). To the best of our knowledge, this is the first report of synthesizing hyperbranched macromers using hydrazide monomers *via* Michael addition approach. The macromers are able to form two types of hydrogels: (1) injectable hydrogels with thiolated hyaluronic acid (HA-SH) through thiol-ene chemistry at physiological conditions, and (2) UV-crosslinked hydrogels in the presence of

photoinitiator. We have investigated the gelation, mechanical properties, degradation profiles and radical scavenging ability of both types of hydrogels. Furthermore, to assess the antioxidant performance of these materials, we evaluated the ROS protection efficiency *in vitro* under high ROS microenvironment. The hydrogels containing disulfide moieties were able to provide excellent antioxidative effect in response to the external ROS, indicating that this versatile strategy allows the fabrication of a new generation of antioxidative biomaterial.

Results and discussion

To synthesize HB-PBHE macromers, we performed Michael addition with PEGDA (Mw = 575 and 700 Da) as A2 and a hydrazide-based monomer - DTP with disulfide bond as B4 (Scheme 1). For comparison, the hydrazide-based monomer SDH without disulfide bond was used (Scheme S1). The molar feed ratio of 2.5:1 (A2:B4) was selected to generate HB-PBHE macromers. The resulting macromers were termed as 575-DTP, 700-DTP, 575-SDH, and 700-SDH, respectively.

Gel permeation chromatography (GPC) was used to monitor the polymerization of monomers with time. Results are shown in Figure S1A-D for DTP macromers and Figure S2A-D for SDH macromers. Number average molecular weight (Mn) and weight average molecular weight (Mw) of all macromers increased gradually and no sign of gelation occurred. Macromers with Mw around 10 kDa and PDI ranged from 1.85 to 2.35 were obtained for further use. The macromers were purified by precipitation in diethyl ether to remove the unreacted monomers. Both proton and carbon nuclear magnetic resonance spectroscopy (1H-NMR and 13C-NMR) were used to confirm the structure of the HB-PBHEs (Figure 1 and Figure S3-5). Typically, in 1H-NMR spectrum of the 575-DTP (Figure 1A), the acrylate protons on terminal group of macromer backbone give signals between 5.90-6.42 ppm. New peaks at 2.84 ppm (e) and 4.15 ppm (c') ppm were attributed to the reacted acrylate groups and terminal PEG units that close to the reacted acrylate groups. Based on the feed ratios and 1H-NMR results, the vinyl content of all macromers were calculated, ranging from 0.62-0.96 mmol/g (Figure S6). All these results demonstrated that "A2+B4" Michael addition is a reliable and reproducible approach for multi-acrylate HB-PBHEs synthesis in a controlled manner.
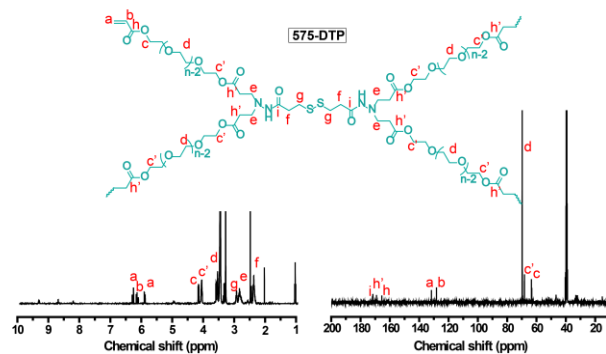

Figure 1. 1H-NMR and 13C-NMR spectra of 575-DTP macromer.

All four macromers were highly water soluble. As previously reported, hydrolytic cleavage facilitates the degrada-

tion of all four macromers in PBS to form small molecules (diol, hydrazide, and acrylate acid).[23] We hypothesize that the disulfide bond-containing HB-PBHEs can undertake both hydrolysis and ROS-triggered degradation. To determine the degradation profile, macromers were dissolved in PBS and H_2O_2 (1 mM) solutions, respectively. The Mw and PDI of the degradation products were monitored by GPC at different time points. The degradation results are shown in Figure 2. As expected, the degradation kinetics of DTP-based macromers exhibit different trends between PBS and H_2O_2 (Figure 2A-B). In H_2O_2 solution, 575-DTP and 700-DTP were fully degraded in 9 days and 22 days, remarkably faster than in PBS (48 days for 575-DTP and 38 days for 700-DTP). In comparison, 575-SDH and 700-SDH showed very similar degradation rates in both PBS and H_2O_2 solutions (Figure 2C-D). Based on these results, the H_2O_2-responsive property of DTP macromers is confirmed. Moreover, DTP-based macromers showed a controlled degradation manner which can realize the adjustable degradation profile of the fabricated hydrogels.

DPPH free radical scavenging assay was used to determine the antioxidative property of HB-PBHEs. Each macromer was tested at a series of concentrations ranging from 0.1-20 mg/mL. The free radical scavenging activity of 575-DTP and 700-DTP macromers increased in a dose-dependent manner up to 66.17% and 58.27% (Figure 3A). Specifically, 575-DTP and 700-DTP, at the same concentration of 5 mg/mL, scavenged 45.47 ± 2.01% and 30.25 ± 2.06% of DPPH radicals within 30 min of incubation. This is significantly higher than that of ascorbic acid (VC) at 0.5 mM (22.97 ± 2.00%, $p<0.01$) (Figure 3B). While only 19.02 ± 1.71% and 12.54 ± 0.92% of the radicals were eliminated by 575-SDH and 700-SDH at the same concentration, respectively. In contrast, ethyl alcohol negative control group resulted in only 0.89% ± 0.06% efficiency. It is worth noting that the moderate antioxidative property of SDH-based macromers is attributed to the residual hydrazide groups (Figure S7) which has been reported previously.[31–33] In order to determine the concentration required to obtain a 50% antioxidative effect (EC_{50}) of the DTP-based macromers, two fitted inhibition curves were obtained based on the inhibition data which gave a 7.24 mg/mL of EC_{50} for 575-DTP and 11.11 mg/mL of EC_{50} for 700-DTP, respectively (Figure 3C-D).

For the development of injectable hydrogels, *in situ* gelation was designed and performed by crosslinking HB-PBHEs with HA-SH *via* thiol-ene click chemistry. Gelation process and mechanical properties were measured by time sweep and strain sweep assessments at different concentrations (Figure 4A-D, Figure S8A-D). The storage modulus (G') represents the energy storage and elastic response of the material. The loss modulus (G") represents the energy loss and viscous properties. G' increased rapidly as gelation proceeded with time at first, then the gel strength kept stable (Figure 4A-B, Figure S8A-B). The strain sweep tests were also employed after G' reached the plateau to monitor the G' and G" in response to the oscillation strain force. The strain sweep data indicated that G' maintains at constant values ranging from 0.1% to 100% for all hydrogels, suggesting that the crosslinking networks hold a broader viscoelastic region during the deformation process (Figure

4C-D, Figure S8C-D). DTP-based hydrogels showed a lower G' compared with SDH-based hydrogels. This difference may be caused by the partial reduction of the disulfide bond in the DTP-based hydrogels by the thiol groups in the HA-SH.

Moreover, the gelation process and rheological properties of UV crosslinked hydrogels were evaluated by time sweep and strain sweep assessments (Figure 4E-H, Figure S9A-D). All HB-PBHEs did not form hydrogels at the concentration of 5% (w/v) owing to the low crosslinking degree so the data were not presented. With 10% and 20% (w/v) concentrations, hydrogels were formed within 60 s of UV irradiation (365 nm) and showed much higher G' compared with HB-PBHE/HA-SH hydrogels. Meanwhile, the viscoelastic regions of all UV crosslinked HB-PBHE hydrogels were narrower than that of HB-PBHE/HA-SH hydrogels due to the increased crosslinking degree.

As the aforementioned data presented, H_2O_2 can be used to manipulate the degradation behavior of DTP-based macromers. To further demonstrate the potential biomedical application, we studied the swelling and degradation profiles to detect H_2O_2-triggered response of DTP-based hydrogels. PBS and H_2O_2 solutions (0.1, 0.5, and 1 mM) were prepared and added to the transwell system containing hydrogels at 37 °C and 150 rpm. Only 1 mM H_2O_2 was used for SDH-based hydrogels as we predicted that the degradation rate will be the same in both PBS and H_2O_2 solutions. As expected, DTP-based hydrogels showed triggered degradation in all H_2O_2 solutions (Figure 5A-D) and degradation time can be manipulated from days to over a month. In comparison, both SDH-based hydrogels showed similar degradation rates in a period of approximately over 40 days in PBS and 1 mM H_2O_2.
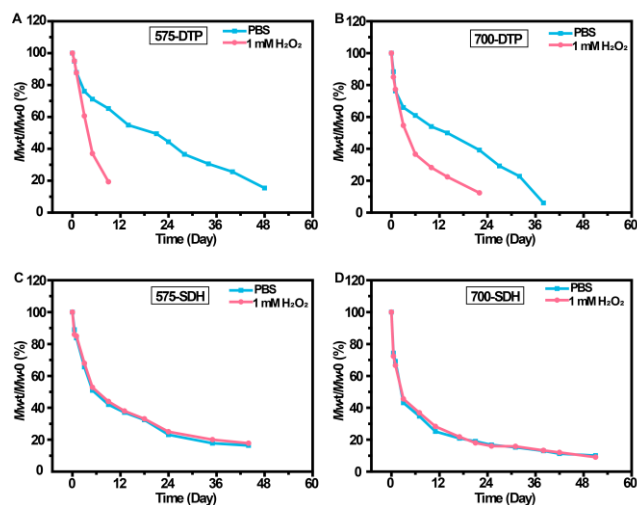

Figure 2. Degradation profile of the four macromers at 20 mg/mL and 37 °C in PBS (blue line) and 1 mM H_2O_2 (pink line). The Mw was monitored by GPC. (A) 575-DTP; (B) 700-DTP; (C) 575-SDH; (D) 700-SDH.
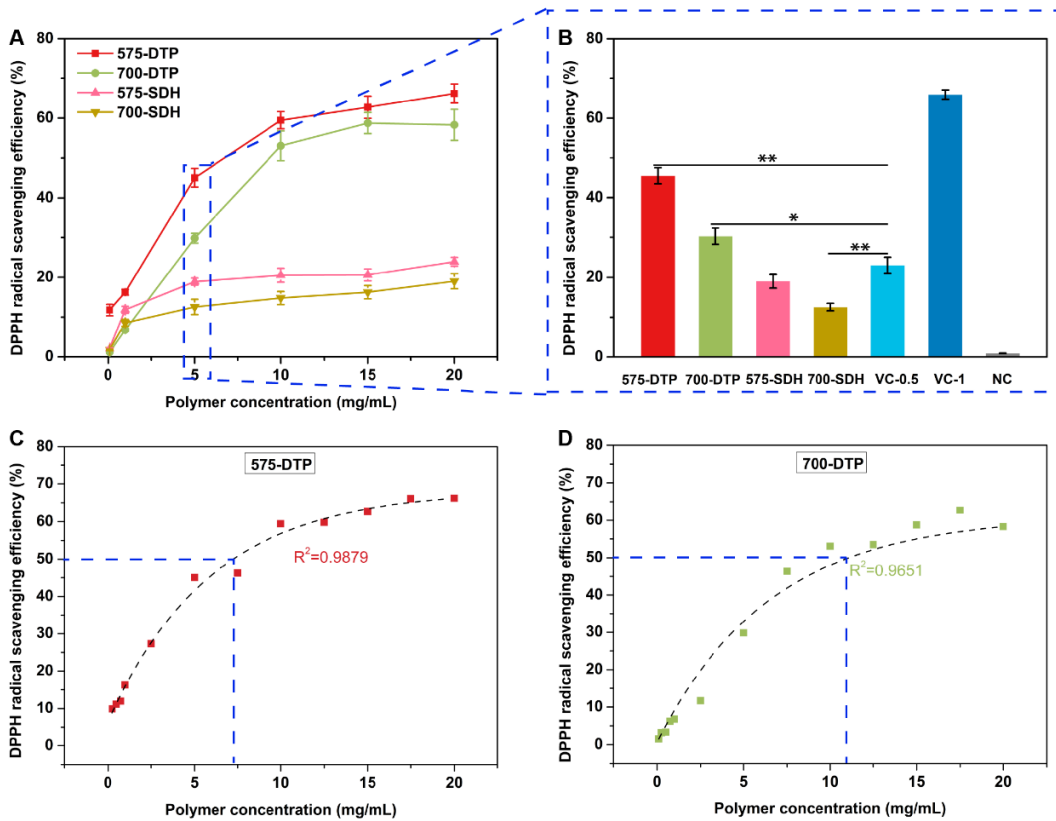
Figure 3. DPPH free radical scavenging assay. (A) DPPH radical scavenging efficiency of different concentrations of HB-PBHEs. (B) DPPH radical scavenging efficiency of HB-PBHEs at 5 mg/mL using VC (0.5 mM and 1 mM) as the positive control and ethyl alcohol as the negative control. (C) and (D) EC_{50} determination of DTP-based macromers. *, $p < 0.05$; **, $p < 0.01$.

The antioxidative ability of the HB-PBHE-based hydrogels was determined by free radical scavenging efficiency using DPPH assay.

The antioxidative ability of HB-PBHE/HA-SH hydrogels with different concentrations was verified first. At 5% and 10% (w/v) macromer concentrations, a significant amount of free radicals (over 80%) were eliminated by 575-DTP/HA-SH and 700-DTP/HA-SH hydrogels, in comparison with 575-SDH/HA-SH and 700-SDH/HA-SH hydrogels which were between 40% to 50% (Figure 6A, $p<0.01$).

Afterwards, HB-PBHE/UV hydrogels with a concentration of 10% were used to scavenge a series of concentrations of DPPH ranging from 25-5000 μm/mL. As shown in Figure 6B, DTP-based hydrogel and SDH-based hydrogel did not show significant difference at 25 μm/mL of DPPH solution. As the concentration of DPPH increased, the scavenging efficiency of all hydrogels decreased while the DTP-based hydrogels still showed considerably higher scavenging capability than SDH-based hydrogels (Figure 6B). These results validated that the free radical scavenging ability was enhanced by introducing the disulfide bond in the HB-PBHE macromers.

Cytotoxicity tests for HB-PBHE macromers were tested by the alamarBlue assay using 3T3 fibroblasts (3T3s) and adipose-derived stem cells (ADSCs). After 24 h co-cultured with a series of macromer concentrations, both cells show high viability over 90% for all four macromers (Figure S10-11).

3T3s and ADSCs were also used for biocompatibility evaluation of the hydrogels using the alamarBlue and live/dead staining methods. Cells were seeded into each of the hydrogels with the final density of $2.5×10^6$ /mL. Figure 7A-D shows that cell viability of both cell lines was above 94% for all hydrogels at 24 and 48 h investigated by the alamarBlue assay. The living status of the cells were confirmed by live/dead staining, which indicated most of the cells were alive (green color) after encapsulated in the hydrogels at 24 h and the gelation process did not induce massive apoptosis (Figure 7E-F). In summary, these hydrogels crosslinked with HA-SH or UV irradiation showed good biocompatibility *in vitro*.

ROS are generated after injuries, which will induce oxidative stress damage in the injury area for both tissues and cells. 575-DTP was selected for the further *in vitro* study of the hydrogel protection under oxidative stress damages due to its remarkable DPPH scavenging ability and 575-SDH was used as the control group (Figure 3). The capacity of 575-DTP-based hydrogels to scavenge ROS was evaluated by using H_2O_2 to mimic the ROS microenvironment that is generated during tissue ischemia.
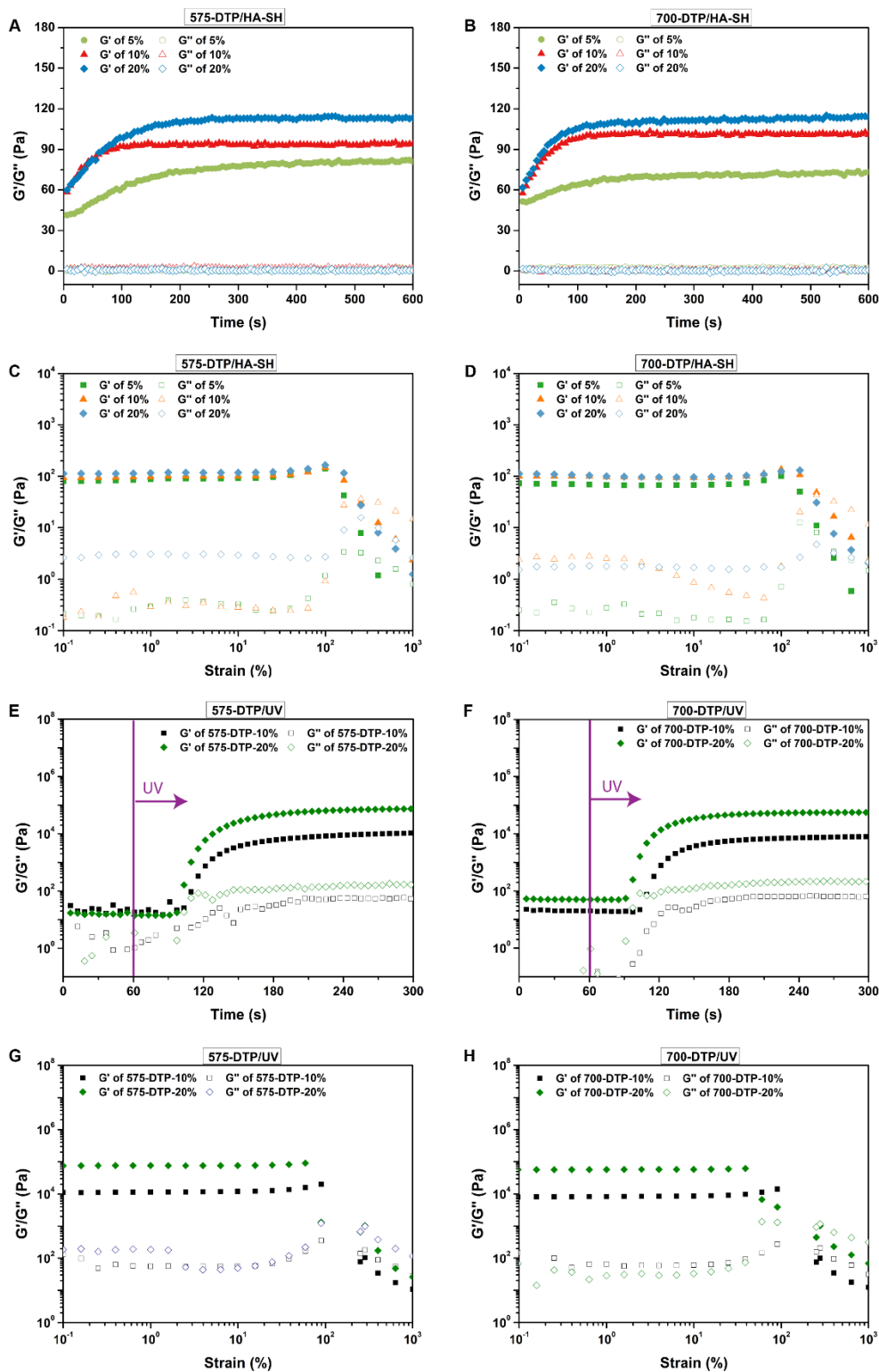
Figure 4. Gelation process and rheological assessments of HB-PBHEs based hydrogels (hydrogels with different concentrations of HB-PBHEs crosslinked with 1% (w/v) HA-SH; hydrogels from UV curing with 0.5% I2959 as the initiator) by rheometry. (A) and (B) time sweep assessments of DTP-based macromers (5%, 10%, and 20% (w/v)) with HA-SH hydrogels at a frequency of 1 Hz and a strain of 1%. (C) and (D) strain sweep assessments (0.1-1000%) of DTP-based macromers with HA-SH hydrogels at a frequency of 1 Hz. (E) and (F) time sweep assessments of DTP-based hydrogels (10%, and 20% (w/v)) crosslinked by UV curing (365 nm) at a frequency of 1 Hz and a strain of 1%. UV irradiation was initiated from 60 s to 180 s. (G) and (H) strain sweep assessments (0.1-1000%) of DTP-based hydrogels (10%, and 20% (w/v)) crosslinked by UV curing (365 nm) at a frequency of 1 Hz.
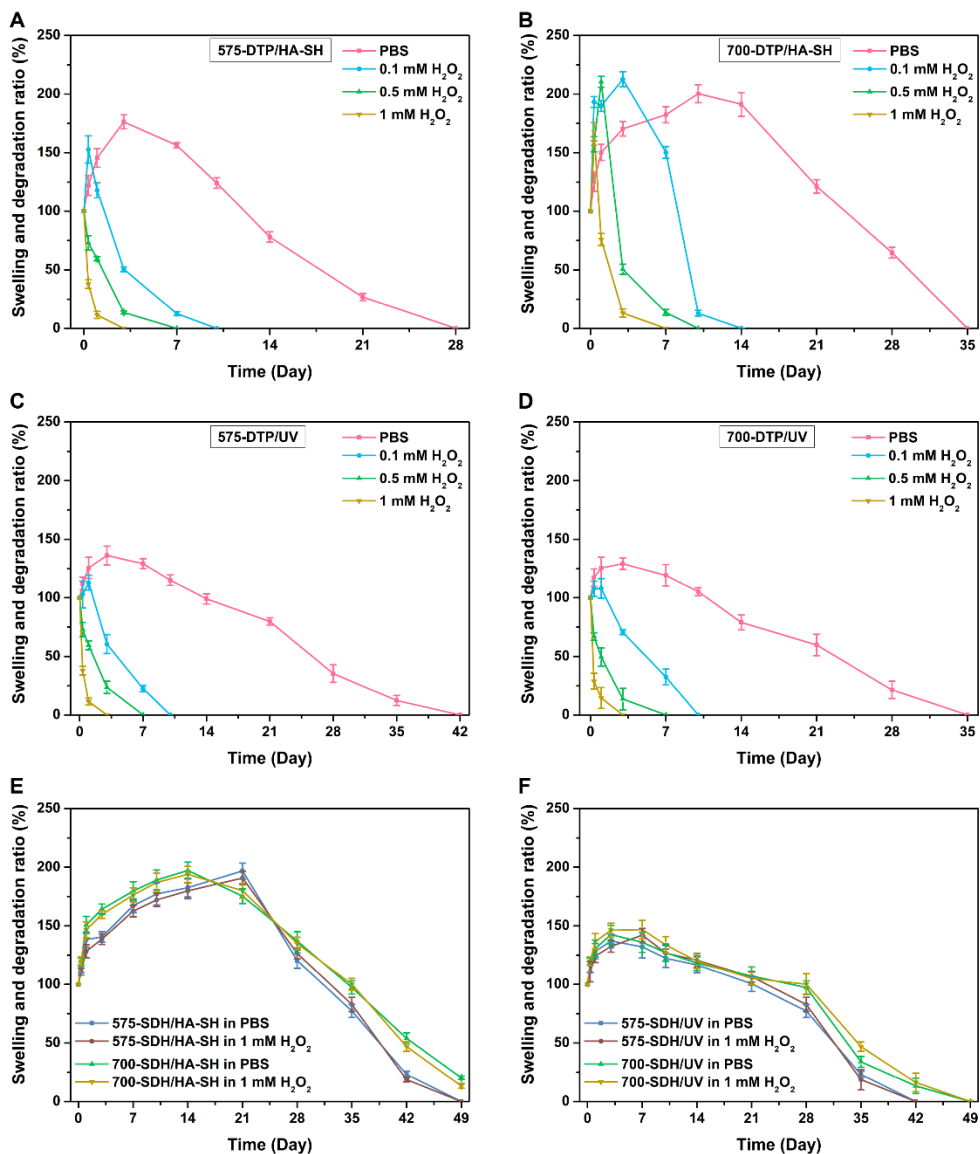
Figure 5. Degradation rates of HB-PBHE based hydrogels in PBS and different concentrations of H_2O_2 at 37 °C. (A) 575-DTP/HA-SH; (B) 700-DTP/HA-SH; (C) 575-DTP/UV; (D) 700-DTP/UV; (E) SDH-based macromer/HA-SH hydrogels; (F) SDH-based macromer/UV hydrogels.

In this study, 0.25 mM H_2O_2 was employed to induce the oxidative stress damage for 3T3s and ADSCs seeded in hydrogels. The efficiencies of the 575-DTP/HA-SH and 575-DTP/UV hydrogels were compared with those of 575-SDH/HA-SH and 575-SDH/UV hydrogels. Significantly improved cell survival was observed for the cells seeded in 575-DTP/HA-SH and 575-DTP/UV hydrogels under oxidative stress microenvironment compared to the control groups (Figure 8A-B). 3T3 cell living status were detected by live/dead staining (Figure 8C). Most of the cells were stained in green, exhibiting living status for 575-DTP/HA-SH and 575-DTP/UV hydrogel encapsulated cells, and so revealing remarkably reduced ROS related damage. While less cells were stained in green in 575-SDH/HA-SH and 575-SDH/UV hydrogels, indicating a lower ROS scavenging capability causing higher cell damage.

The utilization of hydrogel with ROS-induced degradation reduces ROS levels, contributing to therapeutic benefits in anti-inflammation, antioxidant, and anti-cancer.[34] The current study shows the biological significance and strong potential of the newly designed DTP-based HB-PBHE materials for cell protection against oxidant induced damage, which could eventually be useful for antioxidant therapies and radical scavenging protective systems in medical applications.

Conclusion

In summary, a series of new hyperbranched PBHE macromers were designed and synthesized *via* "A2+B4" Michael addition approach between hydrazide-based monomers and PEGDAs. The capability of H_2O_2-triggered degradation can be readily adjusted using DTP monomer with disulfide moieties. Compared with HB-PBHEs synthesized
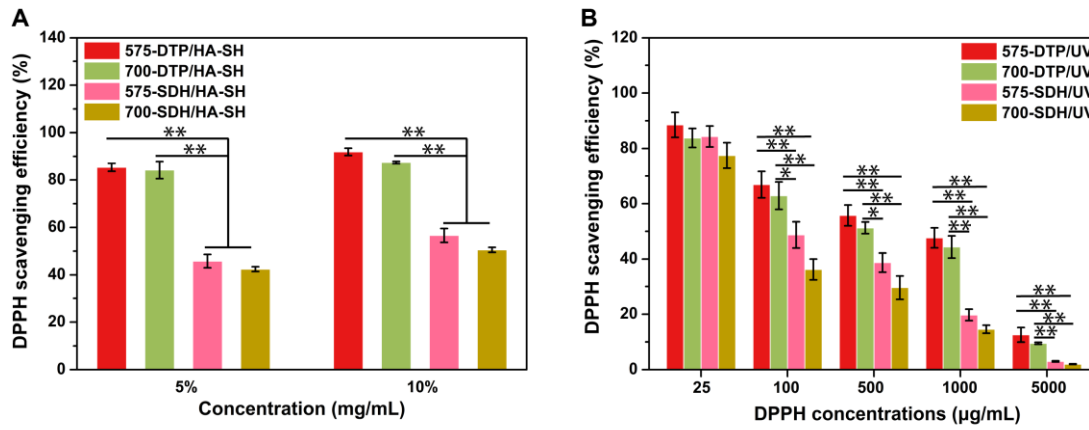
Figure 6. Antioxidative ability of HB-PBHE/HA-SH and HB-PBHE/UV hydrogels. (A) DPPH free radical scavenging ability of HB-PBHE/HA-SH hydrogels. (B) DPPH free radical scavenging ability of HB-PBHE/UV hydrogels with a series of DPPH concentrations. *, $p < 0.05$; **, $p < 0.01$.

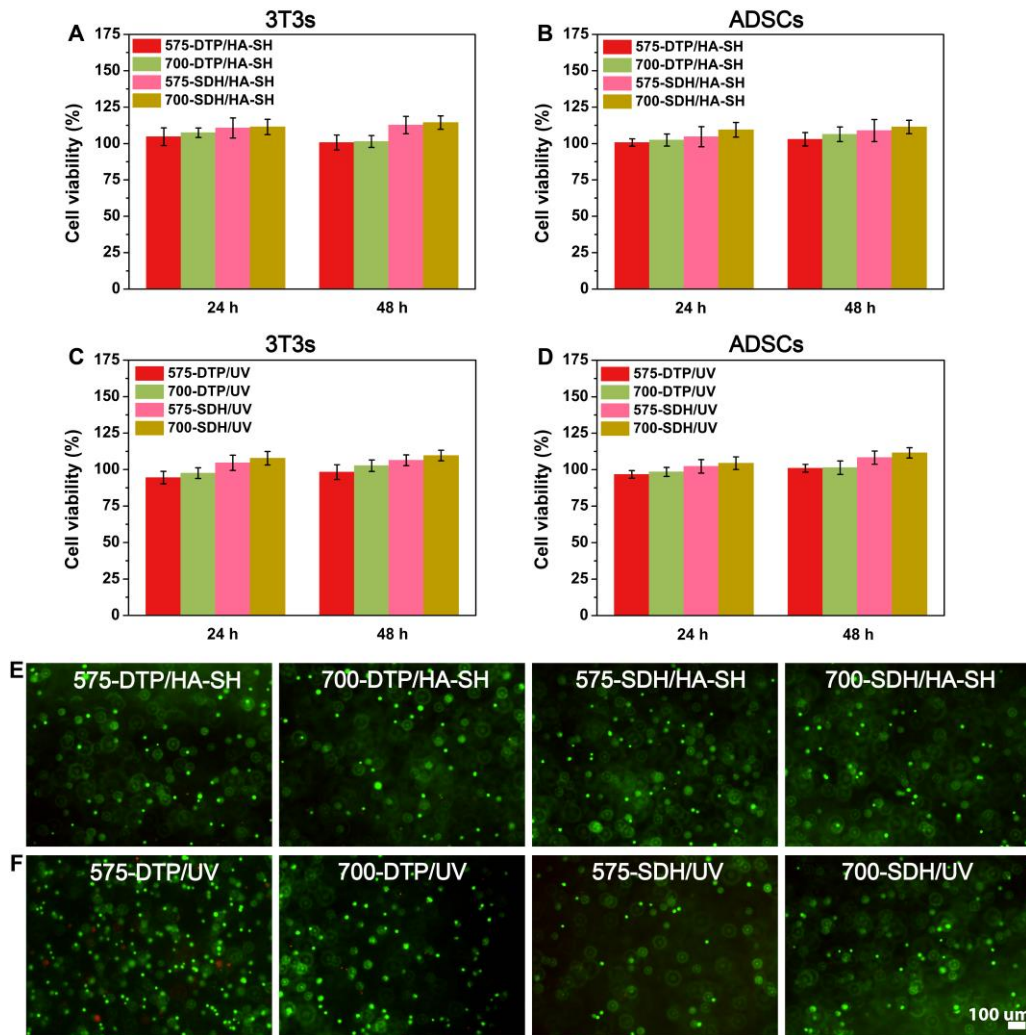**Figure 7.** *In vitro* cell viable analysis of 3T3s and ADSCs in the hydrogels using alamarBlue assay and live/dead images. (A) - (D) cell viability at 24 and 48 h after cell seeded in the hydrogels. (E) and (F) representative live/dead staining images of the 3T3 cell-seeded hydrogels at 24 h (live cells, green color stained with Calcein AM; dead cells, red color stained with ethidium homodimer). Scale bar represents 100 μm.
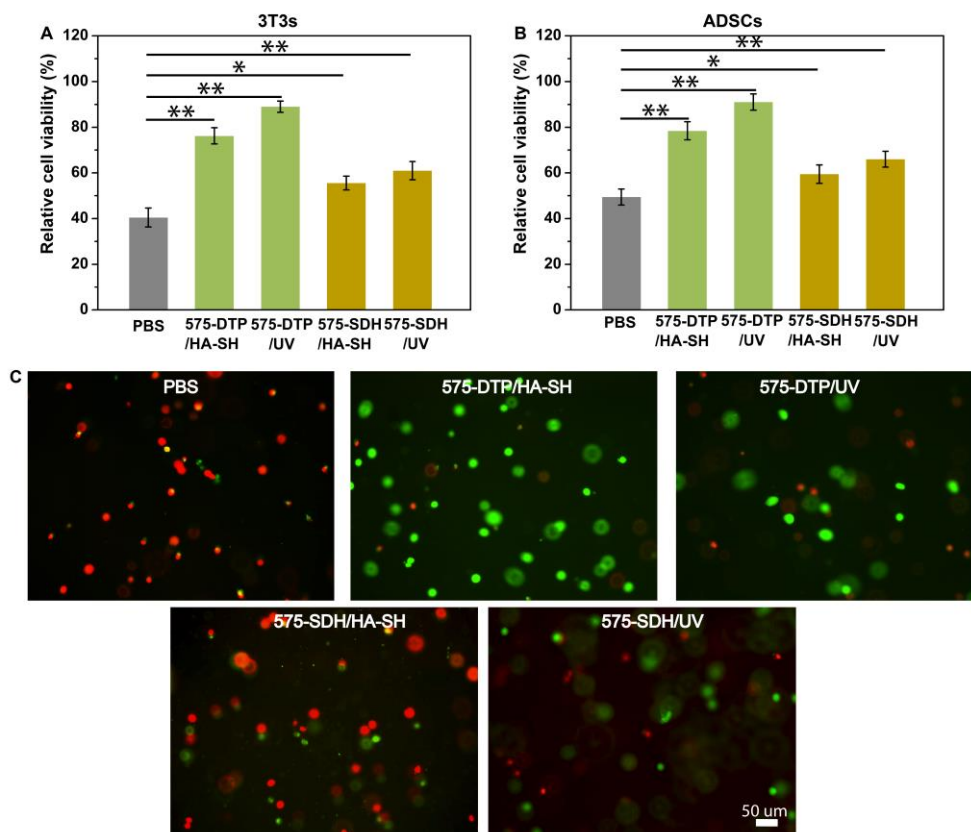
Figure 8. Effect of the 575-DTP and 575-SDH-based hydrogels on ROS protection for 3T3s and ADSCs in the presence of 0.25 mM H_2O_2. (A) and (B) quantitative cell viability from the alamarBlue assay. (C) representative live/dead staining images for 3T3s cell-seeded hydrogels at 24 h. Scale bar, 50 μm. *, $p < 0.05$; **, $p < 0.01$.

from SDH without disulfide, DTP-based HB-PBHEs exhibited a triggered response to H_2O_2 and underwent faster degradation rates. The resultant macromers can form biocompatible hydrogels *via* Michael addition or UV irradiation. DTP-based macromers and hydrogels demonstrated rapid degradation in response to external H_2O_2 and antioxidative ability. Moreover, DTP-based hydrogels showed remarkable ROS protection under high H_2O_2 levels in *in vitro* experiments. Such DTP-based HB-PBHE materials with multi-responsive and high antioxidative efficiency as well as excellent biocompatibility can be used as an efficient ROS-protection platform in a variety of biomedical applications.

Experimental Section

Preparation of Hyperbranched poly(β-amino ester)s (HB-PBHEs)

Four types of HB-PBHEs were synthesized with two types of PEGDA (Mn = 575 and 700 Da) and hydrazide monomers (DTP and SDH) *via* one-pot Michael Addition approach. PEGDA (10 mmol), DTP or SDH (4 mmol), and DMSO (20 ml) were added into a round bottom flask. The reaction was carried out at 90 °C at 700 rpm stirring in an oil bath. The reaction was stopped by taken out from the oil bath and cool to room temperature. The mixed solution was purified by precipitation in excess amount of diethyl ether 5 times and stored in -20 °C freezer before use.

Gel Permeation Chromatography (GPC) characterizations of HB-PBHE macromers

Samples were taken from the reaction flask at regular time points and diluted in DMF and 0.1% LiBr and then filtered through a 0.22 μm filter before analysis. The number average molecular weight (Mn), weight average molecular weight (Mw), and polydispersity index (PDI) were monitored by an Agilent 1260 Infinite GPC system with a refractive index detector (RI). GPC columns (ResiPore 4.6 × 250 mm) were eluted with DMF and 0.1% LiBr. The macromers were analyzed at concentration of 5.0 mg/mL and performed at 80 °C and a flow rate of 1 mL/min.

Proton and carbon nuclear magnetic resonance (^{1}H-NMR and ^{13}C-NMR) characterizations of HB-PBHE macromers

^{1}H-NMR and ^{13}C-NMR analysis were carried out on a 400 MHz Varian NMR system spectrometer and analyzed with MestReNova processing software. The chemical shifts were referenced to the solvent peak of d-DMSO (2.5 ppm for ^{1}H-NMR and 39.52 for ^{13}C-NMR).

Vinyl content and hydrazide content of HB-PBHE macromers

The macromer composition was calculated based on ^{1}H-NMR data from the following equations:

For DTP-based macromers:

Total PEGDA unit: $n = (c + c')/4$ (1)

Vinyl%: v = c/(c + c')   (2)

Total DTP unit: m = f/4   (3)

PEGDA: DTP = n : m   (4)

PEGDA wt% x = *Mw of PEGDA*/((*Mw of PEGDA + Mw of DTP* $\times$ (n/m))   (5)

Vinyl content v = n/m $\times$ 2 $\times$ *v*   (6)

For SDH-based macromers:

Total PEGDA unit: n= (c + c')/4   (7)

Vinyl%: v = c/(c + c')   (8)

Total SDH unit: m = f/4   (9)

PEGDA: SDH = n : m   (10)

PEGDA wt% x = *Mw of PEGDA*/((*Mw of PEGDA + Mw of DTP* $\times$ (n/m))   (11)

Vinyl content v = n/m $\times$ 2 $\times$ *v*   (12)

The TNBS method was used to determine the quantitatively incorporated terminal hydrazide groups into the HB-PBHE macromers. Macromers were dissolved in water (10 mg/mL). Standard samples (*tert*-Butyl carbazate) were prepared and standard curve was used to determine the concentration of hydrazide groups. TNBS work solution (6 mM) was prepared by dilution of original TNBS solution in 0.1 M Sodium tetraborate. Macromer solutions (25 μL) were mixed with TNBS work solution (500 μL) and kept at room temperature for 1 h. Then 50 μL of the mixed sample was determined from the absorbance at 340 nm using quantitative ultraviolet (UV) spectrophotometry in 100 μL HCl (0.5 M).

Degradation of HB-PBHE macromers

All the four purified macromers were highly water soluble. Then macromers were dissolved in PBS with or without 1 mmol H_2O_2 at a concentration of 20 mg/mL, respectively. The prepared solutions were put in 37 °C at 100 rpm. At each time point, 0.5 mL was taken and dissolved in DMF and filtered through an Al_2O_3 pipette to remove phosphate salt. Then the solution was filtered through a 0.22 μm filter for GPC testing.

Degradation percentage was calculated by (Mw-t / Mw-0) $\times$100%   (13)

Mw-0 represents the original Mw of the macromer; Mw-t represents the Mw at scheduled time points.

Radicals scavenging activity of HB-PBHEs

Briefly, DPPH was dissolved in ethanol to make a 25 μM work solution (WS). DPPH standard curve was prepared using a series of concentrations (0, 5, 10, 15, 20, 25 μM). 98 μL of DPPH WS was mixed with 2 μL of a series of macromer solutions (concentration of 0.1, 1, 5, 10, 15, 20 μg/mL). Two positive controls sample were prepared by 2 μL of Ascorbic acid (VC) (5 and 10 mM, respectively) dissolved in PBS. A negative control sample was using only ethanol. All samples were stored at room temperature for 30 min in the dark on a shaker at 200 rpm. Absorbance values were measured at 517 nm using a SpectraMax M3 plate reader (*n* = 3). DPPH (25 mM) served as 100 % radical control, in comparison to the other samples. The concentration of remaining DPPH was determined by the standard curve. The free radical scavenging effect was calculated as the following equation:

Scavenging effect (%) = (1 − (C_{sample}/C_{DPPH})) × 100%   (14)

C_{DPPH} and C_{sample} are the remaining concentrations of DPPH in 100% radical control and the other samples.

EC_{50} determination

Regarding DPPH scavenging assay, the concentration required to obtain a 50% antioxidative effect (EC_{50}) was determined upon the analysis of the macromer concentration-effect curves. Radical scavenging capacity curves were plotted referring to macromer concentrations on the x axis and the relative scavenging ability on the y axis. In this study, OriginPro 8.5 software was used for curve fitting and EC_{50} values processing. The ExpAssoc model was employed for curve fitting to evaluate the EC_{50} radical scavenging value of 575-DTP and 700-DTP macromers, which is expressed as follows:[34]

y = y_0 + A_1 $\times$ (1 - exp(-x/t_1)) + A_2 $\times$ (1 - exp(-x/t_2)) (15)

Where x is the macromer concentrations, y_0, A_1, A_2, t_1 and t_2 are invariant constants. For 575-DTP macromer, the constants obtained from the equation were 6.28508, 31.02653, and 31.02653 for y_0, A_1, A_2, respectively; with a correlation coefficient (R^2) of 0.9879. For 700-DTP macromer, the constants were 0.6001, 30.25963, and 30.25963 for y_0, A_1, A_2, respectively; with a R^2 of 0.9651.

In situ gelation of HB-PBHE macromers with thiolated hyaluronic acid (HA-SH)

Injectable HB-PBHE/HA-SH hydrogels were generated as follows. Firstly, HB-PBHEs were diluted separately within PBS (20% (w/v)) and HA-SH was diluted within PBS (1% (w/v)). Then, 100 mL of diluted HB-PBHE was mixed with 100 μL HA-SH. The mixture was gently vortexed for 10 sec. to obtain a homogeneously distributed solution and form a hydrogel *in situ*.

The gelation process and rheological measurements were carried out by TA Discovery Hybrid Rhemometer. 200 μL prepared solution (100 μL for both HB-PBHEs and HA-SH) was added on a parallel plate (diameter: 20 mm) with a frequency of 1 Hz and a strain of 1%, and the storage modulus (G') and loss modulus (G") were monitored with time. G' and G" values with strain sweeps were also measured.

Rheological measurements of UV crosslinked HB-PBHE hydrogels

Macromer solution was prepared by its dissolution in water (10 or 20% (w/v)) and Irgacure 2959 (0.5 wt%). UV crosslinking was performed with UV generator (Omincure Series 1000 UV) and rheological properties were determined by TA Discovery Hybrid Rhemometer. 200 μL of prepared solution was added on a parallel plate (diameter: 20 mm) with a frequency of 1 Hz and a strain of 1%, and the storage modulus (G') and loss modulus (G") were monitored with time. G' and G" values on various strain sweeps were also measured.

Swelling and degradation properties of HB-PBHE hydrogels

HB-PBHE/HA-SH Hydrogels were prepared by mixing 100 μL HB-PBHEs (10% (w/v)) and 100 μL HA-SH (1% (w/v)) as previously mentioned. HB-PBHE/UV hydrogels was prepared by dissolved HB-PBHEs in 200 μL of water (10 or 20% (w/v)) with Irgacure 2959 (0.5 wt%). UV crosslinking was performed with UV generator (Omincure Series 1000 UV) for 120 s. Transwell permeable insert (BD. Bio Coat, PET track-etched membrane, 3.0 μm) was used to incubate the hydrogels in PBS and H_2O_2 solutions (0.1, 0.5 and 1 mM) at 37 °C at 150 rpm. Weight of samples at regular time points were recorded as W_t, and the initial weight as W_0. Each group had four replicates ($n = 4$).

Swelling ratio was calculated as following equation,

$$\text{Swelling ratio} = W_t / W_0 \times 100\% \qquad (16)$$

Radicals scavenging activity of HB-PBHE based hydrogels

The ability of HB-PBHE/HA-SH hydrogels to act as radical scavengers was conducted. DPPH was dissolved in ethanol with the final concentration of 25 μM. Hydrogels were prepared with the final concentration of 5% and 10% (w/v). 50 μL hydrogel was immersed in 1 mL DPPH solution. The mixtures were continuously shaken in the dark for 30 min, and the absorbance of the solution was measured using SpectraMax M3 plate reader at 517 nm. The solution adding 50 μL PBS without hydrogel was used as the control group. free radical scavenging effect was calculated using the same method as mentioned above. All tests were run in triplicate and averaged.

UV-crosslinked HB-PBHE hydrogels (10%) were prepared as described above, 30 μL each gel. A series of concentration of DPPH solutions was prepared by dissolving DPPH in ethyl alcohol, 25, 100, 500, 1000, 5000 μg/mL. 30 uL of hydrogel was immersed in 1 mL DPPH solution ($n = 3$). 30 uL PBS was used as the control group. The mixtures were continuously shaken in the dark for 30 min. Absorbance values were measured and free radical scavenging efficiency was calculated using the same method as mentioned above.

Cytotoxicity of HB-PBHE macromers

All the macromer solutions for in vitro tests were prepared by PBS buffer and sterilized by 0.2 μm pore size filter. ADSCs and 3T3s were used to test cytotoxicity of macromers. 6.0×10^3 cells were seeded per well and cultured overnight in 96-well plates, respectively. Then the cells were incubated in the condition of different concentrations of HB-PBHEs for 24 h and an alamarBlue test was used to determine both cells' viability ($n = 4$ per group). Cells treated with pure full cell media were used as a positive control (100%). Quantitative data was obtained by monitoring the absorbance of 570/600 nm on a SpectraMax M3 plate reader.

Cytotoxicity of HB-PBHEs/HA-SH and HB-PBHEs/UV hydrogels

The cells were prepared in advance and resuspended in DMEM. Cell suspension was added to HB-PBHE (10% in DMEM) and HA-SH (1% in DMEM) or HB-PBHE (10% in DMEM with 0.5% of I2959) to obtain a final cell density of 2.5×10^6 cells/mL, respectively. HB-PBHE/HA-SH hydrogels were allowed to completely crosslink in the air for 15 min. UV irradiation was used to induce gelation of HB-PBHE/UV hydrogels under 365 nm for 120 sec. 2D cultured cells with the same density was used as the control group (100%). Both 3D and 2D cultured cells were incubated in a 24-well plate at 37 °C with 1 mL full cell media (DMEM with 10% FBS and 1% penicillin/streptomycin) per well ($n = 4$).

AlamarBlue test was used to assess cell viability at 24 and 48 h ($n = 4$ per group) as described above. Briefly, 500 uL of 10% alamarBlue solution in full cell media was added to each well. Data was tested on a plate reader for alamarBlue reduction. Live/dead staining was also performed at 24 h to confirm cell living status as protocol described, calcein AM staining for live cells (green color) and ethidium homodimer-1 for dead cells (red color). Images were taken using an inverted fluorescence microscope (Olympus IX81).

Hydrogel ROS Protection against H_2O_2 induced damage for 3T3s and ADSCs

Cell seeded hydrogels (575-DTP/HA-SH, 575-DTP/UV, 575-SDH/HA-SH and 575-SDH/UV) were prepared as the methods mentioned above. 2D cultured cells were used as the control. Cell density was 2.5×10^6 /mL for both 3D and 2D cultured cells (n = 4). The hydrogels and cells were cultured for 24 h in a 24-well plate with 1 mL fresh cell media. Then the culture media was replaced by 0.25 mM H_2O_2 supplemented DMEM (with 10% FBS and 1% penicillin/streptomycin) before incubated in the 37 °C incubator. The same methods for the alamarBlue and live/dead staining as the previous experiments were used to determine the ROS protection effect of the four hydrogels after 24 h' incubation.

ASSOCIATED CONTENT

Supporting Information. Materials, instrumentation, experimental procedures, supporting figures and tables, and characterization.

AUTHOR INFORMATION

Corresponding Author

* wenxin.wang@ucd.ie
* sigen.a@ucdconnect.ie

Author Contributions

The manuscript was written through contributions of all authors.

Notes
The authors declare no competing financial interest.

ACKNOWLEDGMENT

REFERENCES

(1) Orrenius, S.; Gogvadze, V.; Zhivotovsky, B. Mitochondrial Oxidative Stress: Implications for Cell Death. *Annu. Rev. Pharmacol. Toxicol* **2007**, *47*, 143–183.

(2) Kwon, E. J.; Lo, J. H.; Bhatia, S. N. Smart Nanosystems: Bio-Inspired Technologies That Interact with the Host Environment. *Proc. Natl. Acad. Sci.* **2015**, *112*, 14460–14466.

(3) Xu, Q.; He, C.; Xiao, C.; Chen, X. Reactive Oxygen Species (ROS) Responsive Polymers for Biomedical Applications. *Macromol. Biosci.* **2016**, *16*, 635–646.

(4) Winterbourn, C. C. Reconciling the Chemistry and Biology of Reactive Oxygen Species. *Nat. Chem. Biol.* **2008**, *4*, 278–286.

(5) Newland, B.; Wolff, P.; Zhou, D.; Wang, W.; Zhang, H.; Rosser, A.; Wang, W.; Werner, C. Synthesis of ROS Scavenging Microspheres from a Dopamine Containing Poly(β-Amino Ester) for Applications for Neurodegenerative Disorders. Biomater. Sci. 2016, 4, 400–404.

(6) Huo, M.; Yuan, J.; Tao, L.; Wei, Y. Redox-Responsive Polymers for Drug Delivery: From Molecular Design to Applications. *Polym. Chem.* **2014**, *5*, 1519.

(7) Sun, L.; Liu, J.; Zhao, H. Reactive Polymeric Micelles with Disulfide Groups in the Coronae. *Polym. Chem.* **2014**, *5*, 6584–6592.

(8) Shi, H.; Liu, L.; Wang, X.; Li, J. Glycopolymer–peptide Bioconjugates with Antioxidant Activity via RAFT Polymerization. *Polym. Chem.* **2012**, *3*, 1182.

(9) Feng, C.; Luo, Y.; Nian, Y.; Liu, D.; Yin, X.; Wu, J.; Di, J.; Zhang, R.; Zhang, J. Diallyl Disulfide Suppresses the Inflammation and Apoptosis Resistance Induced by DCA Through ROS and the NF-ΚB Signaling Pathway in Human Barrett's Epithelial Cells. *Inflammation* **2017**, *40*, 818–831.

(10) Chen, D.; Zhang, G.; Li, R.; Guan, M.; Wang, X.; Zou, T.; Zhang, Y.; Wang, C. R.; Shu, C.; Hong, H.; Wan, L. Biodegradable, Hydrogen Peroxide and Glutathione Dual Responsive Nanoparticles for Potential Programmable Paclitaxel Release. *J. Am. Chem. Soc.* **2017**, 10–13.

(11) Trombino, S.; Cassano, R.; Bloise, E.; Muzzalupo, R.; Tavano, L.; Picci, N. Synthesis and Antioxidant Activity Evaluation of a Novel Cellulose Hydrogel Containing Trans-Ferulic Acid. *Carbohydr. Polym.* **2009**, *75*, 184–188.

(12) Nakagawa, H.; Matsumoto, Y.; Matsumoto, Y.; Miwa, Y.; Nagasaki, Y. Design of High-Performance Anti-Adhesion Agent Using Injectable Gel with an Anti-Oxidative Stress Function. *Biomaterials* **2015**, *69*, 165–173.

(13) Lai, J. C. Y.; Lai, H. Y.; Rao, N. K.; Ng, S. F. Treatment for Diabetic Ulcer Wounds Using a Fern Tannin Optimized Hydrogel Formulation with Antibacterial and Antioxidative Properties. *J. Ethnopharmacol.* **2016**, *189*, 277–289.

(14) Sahiner, N.; Sagbas, S.; Sahiner, M.; Silan, C.; Aktas, N.; Turk, M. Biocompatible and Biodegradable Poly(Tannic Acid) Hydrogel with Antimicrobial and Antioxidant Properties. *Int. J. Biol. Macromol.* **2016**, *82*, 150–159.

(15) Zhang, Y. S.; Khademhosseini, A. Advances in Engineering Hydrogels. *Science (80-.).* **2017**, *356* 6337.

(16) Anderson, D. G.; Tweedie, C. A.; Hossain, N.; Navarro, S. M.; Brey, D. M.; Van Vliet, K. J.; Langer, R.; Burdick, J. A. A Combinatorial Library of Photocrosslinkable and Degradable Materials. *Adv. Mater.* **2006**, *18*, 2614–2618.

(17) Lynn, D. M.; Langer, R. Degradable Poly(β-Amino Esters): Synthesis, Characterization, and Self-Assembly with Plasmid DNA. *J. Am. Chem. Soc.* **2000**, *122*, 10761–10768.

(18) Akinc, A.; Zumbuehl, A.; Goldberg, M.; Leshchiner, E. S.; Busini, V.; Hossain, N.; Bacallado, S. a; Nguyen, D. N.; Fuller, J.; Alvarez, R.; Borodovsky, A.; Borland, T.; Constien, R.; de Fougerolles, A.; Dorkin, J. R.; Narayanannair Jayaprakash, K.; Jayaraman, M.; John, M.; Koteliansky, V.; Manoharan, M.; Nechev, L.; Qin, J.; Racie, T.; Raitcheva, D.; Rajeev, K. G.; Sah, D. W. Y.; Soutschek, J.; Toudjarska, I.; Vornlocher, H.-P.; Zimmermann, T. S.; Langer, R.; Anderson, D. G. A Combinatorial Library of Lipid-like Materials for Delivery of RNAi Therapeutics. *Nat. Biotechnol.* **2008**, *26*, 561–569.

(19) Yang, F.; Cho, S. W.; Son, S. M.; Bogatyrev, S. R.; Singh, D.; Green, J. J.; Mei, Y.; Park, S.; Bhang, S. H.; Kim, B. S.; Langer, R.; Anderson, D. G. Genetic Engineering of Human Stem Cells for Enhanced Angiogenesis Using Biodegradable Polymeric Nanoparticles. *Proc Natl Acad Sci U S A* **2010**, *107*, 3317–3322.

(20) Zhou, D.; Wang, W.; Cutlar, L.; Gao, Y.; Wang, W.; O'Keeffe-Ahern, J.; McMahon, S.; Greiser, U.; Duarte, B.; Larcher, F.; Rodriguez, B. J. The Transition from Linear to Highly Branched Poly(β-Amino Ester)s: Branching Matters for Gene Delivery. *Sci Adv* **2016**, *2*, e1600102.

(21) Nutan, B.; Chandel, A. K. S.; Bhalani, D. V.; Jewrajka, S. K. Synthesis and Tailoring the Degradation of Multi-Responsive Amphiphilic Conetwork Gels and Hydrogels of Poly(β-Amino Ester) and Poly(Amido

Amine). *Polym. (United Kingdom)* **2017**, *111*, 265–274.

(22) Poly, T.; Zhang, Y.; Wang, R.; Hua, Y.; Baumgartner, R.; Cheng, J. Trigger-Responsive Poly(β -Amino Ester) Hydrogels. *ACS Macro Lett.* **2014**, *3*, 693–697.

(23) Xu, Q.; Guo, L.; Sigen, A.; Gao, Y.; Zhou, D.; Greiser, U.; Creagh-Flynn, J.; Zhang, H.; Dong, Y.; Cutlar, L.; Wang, F.; Liu, W.; Wang, W.; Wang, W. Injectable Hyperbranched Poly(β-Amino Ester) Hydrogels with on-Demand Degradation Profiles to Match Wound Healing Processes. *Chem. Sci.* **2018**, *9*, 2179–2187.

(24) Beidler, S. K.; Douillet, C. D.; Berndt, D. F.; Keagy, B. A.; Rich, P. B.; Marston, W. A. Inflammatory Cytokine Levels in Chronic Venous Insufficiency Ulcer Tissue before and after Compression Therapy. *J. Vasc. Surg.* **2009**, *49*, 1013–1020.

(25) Schreml, S.; Szeimies, R. M.; Prantl, L.; Karrer, S.; Landthaler, M.; Babilas, P. Oxygen in Acute and Chronic Wound Healing. *Br. J. Dermatol.* **2010**, *163*, 257–268.

(26) Lee, C. C.; MacKay, J. a; Fréchet, J. M. J.; Szoka, F. C. Designing Dendrimers for Biological Applications. *Nat. Biotechnol.* **2005**, *23*, 1517–1526.

(27) Zhou, D.; Pierucci, L.; Gao, Y.; O'Keeffe Ahern, J.; Huang, X.; Sigen, A.; Wang, W. Thermo- and PH-Responsive, Coacervate-Forming Hyperbranched Poly(β-Amino Ester)s for Selective Cell Binding. *ACS Appl. Mater. Interfaces* **2017**, *9*, 5793–5802.

(28) Cutlar, L.; Zhou, D.; Gao, Y.; Zhao, T.; Greiser, U.; Wang, W.; Wang, W. Highly Branched Poly(β-Amino Esters): Synthesis and Application in Gene Delivery. *Biomacromolecules* **2015**, *16*, 2609–2617.

(29) Zhou, D.; Gao, Y.; Aied, A.; Cutlar, L.; Igoucheva, O.; Newland, B.; Alexeeve, V.; Greiser, U.; Uitto, J.; Wang, W. Highly Branched Poly(β-Amino Ester)s for Skin Gene Therapy. *J. Control. Release* **2016**, *244*, 336–346.

(30) Lakes, A. L.; Jordan, C. T.; Gupta, P.; Puleo, D. A.; Hilt, J. Z.; Dziubla, T. D. Reducible Disulfide Poly(Beta-Amino Ester) Hydrogels for Antioxidant Delivery. *Acta Biomater.* **2018**, *68*, 178–189.

(31) Shen, W.; Qiu, Q.; Wang, Y.; Miao, M.; Li, B.; Zhang, T.; Cao, A.; An, Z. Hydrazine as a Nucleophile and Antioxidant for Fast Aminolysis of RAFT Polymers in Air. *Macromol. Rapid Commun.* **2010**, *31*, 1444–1448.

(32) Packiaraj, S.; Pushpaveni, A.; Govindarajan, S.; Rawson, J. M. Structural and Anti-Oxidant Properties of Guanidinium Pyrazole-3,5-Dicarboxylates. *CrystEngComm* **2016**, *18*, 7978–7993.

(33) Ogata, S.; Takeuchi, M.; Teradaira, S.; Yamamoto, N.; Iwata, K.; Okumura, K.; Taguchi, H. Radical Scavenging Activities of Niacin-Related Compounds. *Biosci. Biotechnol. Biochem* **2002**, *1*, 641–645.

(34) Wang, C.; Wang, J.; Zhang, X.; Yu, S.; Wen, D.; Hu, Q.; Ye, Y.; Bomba, H.; Hu, X.; Liu, Z.; Dotti, G.; Gu, Z. In Situ Formed Reactive Oxygen Species–responsive Scaffold with Gemcitabine and Checkpoint Inhibitor for Combination Therapy. *Sci. Transl. Med.* **2018**, *10*, eaan3682.

TOC